Al-Rafidain Engineering Journal (AREJ) Vol.28, No.1, March 2023, pp. 256-271

The Experimental Investigation of Double -Pass Solar Air Heater with V-Corrugated Plate, Phase -Change Material and Baffles Under Recycling Operation

Omar Mohammed Hamdoon*
eng.omar.m.hamdoon@uomosul.edu.iq

Ibrahim Ababakr Ali**
ibrahim.ababakr@gmail.com

*Mechanical Engineering Department, Collage of Engineering, University of Mosul, Mosul, Iraq
** Energy Engineering Department, Technical College of Engineering, Duhok Polytechnic University, Duhok, , Iraq

Received: 2022-09-21 Received in revised form: 2022-10-25 Accepted: 2022-11-15

ABSTRACT

The current paper presents an experimental work that had been implemented to observe the performance of an improved solar air heater and compared it with that of a conventional double-pass flat plate solar air heater. Improvements that have been added include the use of a V-shaped corrugated plate at an angle of 60 degrees, the addition of wood baffles in the lower pass and the use of phase-changing materials PCM as well as air recycling conditions. The heater was designed and tested under the weather conditions prevailing in the Duhok Governorate (latitude 36° 52' 1.52" N and longitude 42° 59' 18.42" E) in the Kurdistan Region of Iraq. The phase-changing material PCM is paraffin wax. The gathered results showed that the improvements that were added to the solar air heater significantly improved the performance at different mass flow values (0.037, 0.057, 0.077 kg/sec). For example, the maximum values of useful heat transfer at mass flow rates (0.037, 0.057, and 0.077kg/s) are 1.68, 1.86, and 2.34 kW, respectively, and the daily efficiency for improving and conventional heater value at mass flow rate 0.037kg/s for 15,16, and 17 of February on 2022 was (84% and 45%), (86% and 46%), and (91% and 60%), respectively.

Keywords:

Solar Air Heater, PCM, recycle rate, V- corrugated absorber plate.

1. INTRODUCTION

The purpose of a solar air heater (SAH) is to convert the solar energy into useful thermal energy. In general, the solar air heater acts as a device that transfer heat to the air passing through a system. The thermal efficiency of solar air heater is influenced by different factors, such as solar radiation, the method of design of the heater, the space and design of the absorber area, the temperature of the air inside the heater and the mass flow rate of the air. The solar air heater is generally used for energy production from low to moderate temperatures. These kinds of heater systems are good and easy to maintain, but they have low thermal efficiency defects [1]. Solar air heaters are widely used in a variety of applications, including drying agricultural goods, space heating, curing industrial items and wood heating architecture, and high-density desalination [2]. Many researchers do their will to enhance the performance of solar air heaters by changing the design of the collector and using phase change materials as an energy storage system.

Muhammad Sajawal et al. [3] conducted an experiment work in order to enhance the thermal performance of a double-pass solar air heater considering phase -change materials (PCMs) and finned tubes. Three cases were adopted, in the first case no PCM was used, while in the second case, a phase -change material (RT44HC) with a high melting point was used.

Finally, in the third case, a configuration containing (RT44HC) and (RT18HC) were investigated. The obtained results showed that the average thermal efficiencies for the first, second, and third configurations are 53.2%, 68.4%, and 71.9%, respectively.

Aymen EL KHADRAOUI et al. [4] carried an experimental work to observe the daily efficiency of the solar air heater (SAH) by utilizing thermal heat storage which is paraffin wax. Two different arrangements were tested, the first arrangement without (PCMs) and the second one with (PCMs). The author claimed that the daily efficiency of the solar heater (SAH) with PCM was nearly 33%, while the outlet air temperature was increased after sunset with (PCMs), and the daily efficiency value without PCM was 17%.

A.E. Kabeel et al. [5] conducted an experimental study to investigate the thermal performance of finned plate solar air heater (FPSAH) during the daily time, and also investigate its behavior under changing of mass flow rate using PCM such as paraffin wax. The author and his colleague were found that the daily efficiency was increased when the mass flow rate of air increased with and without PCM as paraffin wax. It was seen that the outlet temperature decreased. As well as the FPSAH operation lasted up to 4 hours during night time, with PCM FPSAH enhances daily efficiency about 10.8-13.6 percent when they used with the PCM.

A.E. Kabeel et al. [6] carried an experimental work on a flat and V-corrugated plate of SAHs with built-in PCM as thermal energy storage material using paraffin wax. The factors influencing the thermal performance of the flat and V-corrugated plate with and without PCM were considered. The experimental results showed that when the PCM was used, the outlet temperature of the V-corrugated plate solar air heater is rises from 1.5–7.2 °C, which is higher than the ambient temperature for 3.5 hours after sunset, compared to 1–5.5 °C for 2.5 hours after sunset for the flat plate solar air heater. When the mass flow rate is 0.062 kg/s, and the daily efficiency of the V-corrugated with PCM was 12% higher than the corresponding ones without PCM, and it was 15% and 21.3 % higher than the corresponding values when the flat plate was used with and without PCM respectively at mass flow rate was 0.062 kg/s.

Abdulrahman Shakir Mahmood, [7] investigated the performance of a double -pass solar air heater with and without PCM as a paraffin wax to evaluate the effect of charging and discharging characteristics of two same design of the SAHs at a fixed of air mass flow 0.0375 kg/s. They found that the outlet air temperature and daily efficiency were increased with time about (1.5 – 6.5 °C after sunset for 5 hours The researcher and his groups noted the amount of daily efficiency was improved with and without PCM of the heater 54% and 47% respectively.

Ahmet Koca et al. [8] examined the performance of a flat-plate solar collector with a PCM-filled tank. An energy and exergy analysis was implemented. TES as $CaCl_2$. $6H_2$ to enhance the energy and exergy efficiencies was considered. They showed that the average net efficiency of the energy and exergy analysis was 45% and 2.2% respectively.

Ramin Moradi et al. [9] utilized PCM to maximize charging and heat recovery. The impacts of three factors on SAH performance were investigated numerically. Only one operating parameter was changed while the other two were maintained constant. The second variable was then changed while the third remained constant and the first was kept at the prior step's near-optimal value. The third variable was the same. Experimented confirmed a transient 2-D laminar model accessible in Fluent 17's CFD code. The tests also created affordable PCM packaging that was successful in heat transmission to the PCM. The result showed, that the SAH was able to preserve the average nightly temperature differential at 4.5 °C using 23.5 kg of paraffin (4 cm thick layer under the absorber plate) and a total energy efficiency of around 37% at a 65 kg/h air -flow rate.

V. V. Tyagi et al. [10] presented a thermal analysis to examine the performance of a solar air heater experimental work with and without phase- change material (PCM), namely, paraffin wax and hytherm oil were considered. However, to compare the performance of this system, it was set up without PCM, with PCM, and with hytherm oil. Paraffin wax has a higher exit temperature than hytherm oil. Also, without thermal energy storage with TES is examined. Results show that there was no energy gain in the evening, but with TES, there was a heat gain of roughly four hours, which makes the system last for a four-hour.

A.F. Sharol et al. [11] investigated the effect of the TES material experimentally of DPSAH with cross-matrix absorber CMA. The arrangements are considered with and without DPSAH_CMA. The comparison was carried out for surrounding conditions in which the DPSAH-CMA-with PCM achieved greater thermal efficiency by 17 percent compared to DPSAH-CMA-without PCM. For the DPSAH-CMA-with PCM and without PCM. Results showed that the exergy efficiency was nearly 23% and 15%, respectively.

Rajendra Karwa et al. [12] presented an experimental work to assess the amount of heat transfer and friction in a rectangular section duct with completely perforated baffles (open area ratio 46.8%) or half perforated baffles (open area ratio 26%) attached to one of the larger sides at a relative roughness pitch of 7.2–28.8. The study demonstrates an increase in Nusselt number of 79–169% over the smooth duct for fully perforated baffles and 133–274 % for half perforated baffles, while the friction factor for fully perforated baffles was 2.98–8.02 times that of the smooth duct and 4.42–17.5 times that of the half-perforated baffles. By and large, half perforated baffles perform better thermos-hydraulically than completely perforated baffles of the same pitch. Of all the designs investigated, half perforated baffles with a relative roughness pitch of 7.2 provide the biggest performance benefit (51.6–75%) over a smooth duct with identical pumping power.

Ensaci et al. [13] conducted an experimental and theoretical study to investigate the baffles location in the air path in order to enhance the thermo-hydraulic performance of the SAH. The researcher discovered that the optimum thermo-hydraulic performance factor is achieved in the case where the baffles are located in the first part of the air channel which occupies 50% of the solar air heater.

Hassan Olfian et al. [14] examined numerically two different types of baffles located in the gap of the SAH. System. The rectangular angle in the lower gap and V- shaped angle in the upper gap of the ducts, was tested with and without baffles at different angles at Reynold number Re=2000. Results showed the thermal efficiency for using baffles for the angle (90°, 60°, and 45°) of V-shaped angled baffles are 27%, 18%, and 13% respectively , which is greater than no baffles in the gap at the same Reynolds number.

Ramadhani Bakari [15] studied flat plate solar collectors integrated with varying numbers of baffles. The efficiency of an air flat plate solar collector integrated with 2, 3, 4, and 8 baffles was investigated and compared to that of a conventional collector in this experiment. It can be observed, the collector with four baffles maintained a higher temperature throughout the day than the collector with two or three baffles. The model with four baffles produced an average temperature of 42.7 degrees Celsius, whereas the models with two, three, and no baffles produced 42.1° C, 41.6°C and 40.1° C, respectively. On the other hand, the greatest temperature obtained in the collector with four baffles was 52.2° C, whereas the collection with two, three, or no baffles reached 50° C, 51° C, and 48° C, respectively.

Chii-Dong Ho et al. [16] carried an experimental and theoretical work to estimate the performance of the SAH of double -pass V-corrugated under recycle. Results show the thermal efficiency can be improved with different operation parameter for both the V-corrugated and flat plate. Under various recycle ratios and mass flow rates, the results reveal that the collector efficiency increase of the recycling double-pass V-corrugated operation was substantially larger than that of the other configurations. The results demonstrate that by made a V-corrugated absorber plate in the conduit to conduct a recycling double-pass operation, collector efficiency was improved, particularly while operating at lower air mass flow rates. When the air mass flow rate and/or the recycling ratio rise, the collector efficiency improves further.

Chii-Dong Ho et al. [17] examined the performance of a solar air heater with a double-pass design as well as fin and baffle designs. The influence of the recycling procedure was studied using both experimental and theoretical methods. Under varied reflux ratios and mass flow rates, the collector efficiency of the finned plus baffled double-pass with recycling design is significantly higher than the other designs. When both collector efficiency and pumping power requirements are taken into account, the ideal reflux ratio for the fined plus baffled double-pass design is around 0.5. For double-pass operation, an economic consideration in terms of heat transfer efficiency and power consumption increase.

The current paper presents an experimental work, the performance of a double pass solar air heater with integrated storage unit is evaluated. The calendrical pipe of copper was filled with paraffin wax is used as a phase - change energy storage material. Charging and discharging experiments had been conducted and the performance results obtained in the solar air heater with PCM, corrugated absorber plate, baffles and conventional solar air heater are compared under the same climatic conditions in Duhok Governorate/ Kurdistan region/ Iraq.

2. Thermal performance

The thermal efficiency of a SAH may be defined as the ratio of useable heat obtained by the solar collector to solar radiation falling on the collector's surface [18]. Hence, the thermal efficiency of a SAH can be written as follows:

$$\eta_{th} = \frac{\dot{Q}_u}{\dot{Q}_c} \quad (1)$$

Where $\dot{Q}_c$ denotes the solar radiation hitting on the surface of the solar SAH:

$$\dot{Q}_c = I * A_c \quad (2)$$

The solar radiation falling per unit area of the collecting surface is referred to I and A_C is the collector surface area. $\dot{Q}_u$ represents the heat transferred from the solar air heater (useful gain of heat carried away by air) to the flowing air.

$$\dot{Q}_u = \dot{m} C_p \, \Delta T \quad (3)$$

Where:

$\dot{m}$: air mass flow rate in (kg/s)

C_p: air-specific heat in (kJ/kgK)

ΔT: the difference of air temperature in C°

$\Delta T = T_{out} - T_{in}$

T_{out}: the outlet air temperature form SAH in C°

T_{in}: the inlet air temperature (ambient temperature) in C°

$\dot{m} = \rho_{air} * A_t * V_{air}$

ρ_{air} = density of the air kg/s

V_{air} = air speed exit from the heater m/s

A_t = cross section air of exit air the heater m^2

As a result, the solar air heater's thermal efficiency can be stated using the following formula.

$$\eta_{th} = \frac{\dot{m} * C_p (T_{out} - T_{in})}{I * A_c} \quad (4)$$

The daily efficiency of the heater was determined by the below equation (5).

$$\eta_D = \frac{\sum \dot{Q}u}{\sum I * A_c} \quad (5)$$

3. Experimental setup:

3.1 The structure of solar air heater SAH

Solar air heaters dimensions of 2 m in length, 1 m in width, and 0.75 m height were made from mahogany wood with a thickness of 20 mm. An aluminum sheet of 0.7 mm is used to separate the upper passes from lower passes of the SAHs. Insulation materials, such as foam of 20 mm were used in order to reduce the heat transfer from the bottom and sides of collectors.

Two collectors from the top side are covered by a glass thickness of 6 mm to preserve a steady distribution inside the collector. Utilizing an axial fan, the air is forced through the upper channel between the glass cover and the absorber (corrugated or flat) plate and then changes direction at the end of the passage to enter the lower pass between the absorber plate and the back cover, which is also made from wood. The SAHs-based main frame is held by a base angle iron of 4 mm in thickness to tilt the solar heater at a fixed angle of 55° in the south direction in the polytechnic university, technical college of engineering in Duhok city.[19] More details are shown in table 1.

Table 1: Parameters used in solar collector validation

Specifications	Detail
Glass cover thickness	6 mm
Area of the absorber flat plate for conventional SAH	2 m2
Area of the absorber V-corrugated plate for improved SAH	3.88 m2
Lower and upper pass height	75 mm
Insulation thickness	Bottom and side thickness 20 mm
Outside diameter of pipe	22 mm
Inside diameter of pipe	20 mm
Length of one pipe	1 m
Total number of pipes	20 pipes
Total length of pipe	20 meters
Number of thermocouples for conventional SAH	14 thermocouples
Number of thermocouples for improved SAH	17 thermocouples
Axil fan	3 fans for each system
Phase change materials	0.208 kg for each pipe

In the current study, three main additions were made to improve the performance of the solar air heater. This includes using a V-shaped corrugated absorber plate to increase the surface area, and adding baffles in the lower pass to increase the turbulence and thus increase the rate of heat transfer. Finally, placing phase -change materials (Paraffin wax) in tubes in the lower pass of the collector to store extra heat for use when the solar radiation is unavailable during the night and cloudy days The solar heater was operated using recirculating air, and the ratio of recirculated air to total air was R=0.55, Figure 1.

Fig. 1 copper pipes location.

Paraffin wax has been used as a phase -change material to store heat energy because it is available, cheap, has high-capacity storage, and is chemically stable compared to other materials. It is also capable to transfers heat from hot pipes to the air in a lower gap, and to increase the temperature of the air in the channel and the outlet temperature for an improved system of the solar air heater. In the discharge process, the outlet temperature of SAH with PCM has the highest value compared with SAH and without PCM. Paraffin wax is placed in the 20 pipes of copper with dimensions of 20 mm inner diameter, 22 mm outer diameter, and 1 meter in length of copper pipe were arranged and fixed horizontally in the heater and classified in three groups. The first group was in the bottom of the heater is called pipes1, the second group in the middle group is named pipes2 and the last group arrangement at the top of the heater is called pipe3, figure 2 explains copper pipe fill by PCMs, were used to store energy, especially after sunset. The physical properties of paraffin wax are given in table2.

Fig. 2. Explain copper tubs fill its by paraffin wax

Table 2: Thermo Physical properties of paraffin wax

Melting Point	38-43	[°C]
Congealing area	43-37	[°C]
Heat storage capacity ±7.5%	165	[kJ/kg]
Specific heat capacity	2	[kJ/kgK]
Density solid at 15oC	880	[Kg/m3]
Density liquid at 80oC	760	[Kg/m3]
thermal conductivity (both phase)	0.2	[W/(m*K)]
Volume expansion	12.5	[%]
Flash point	186	[°C]
Max. operation temperature	72	[°C]

The absorber is made of an aluminum plate and its colure is changed to black in order to absorb nearly most falling solar radiation. While the thermocouples of type (K) are used to read the temperatures at a different location in the SAHs system and connect them with a data logger to store data, knowing that the number of thermocouples connected with the data logger is (31) thermocouples, 14 and 17 for conventional and improved SAHs, respectively. The thermocouples have been located on the conventional system with three thermocouples for the lower and upper gaps to measure the air temperature, three thermocouples for the absorbent plate, and glass cover to measure the temperature of the plate and glass respectively, as well as a thermocouple to measure the temperature of the inlet air of the SAH and another for measuring the outlet temperature of SAH. As for the improved solar air heater, the thermocouples were installed in the same places that they were installed for the conventional heater, except for three additional thermocouples, which were installed on the tubes that contain PCM which is paraffin wax, to measure the temperature of the pipes. The figure 3 shows the thermocouple installation. Pyranometer was used to measure the solar intensity (*I*) in units of W/m^2. The improved and conventional SAH are depicted in Figure (4).

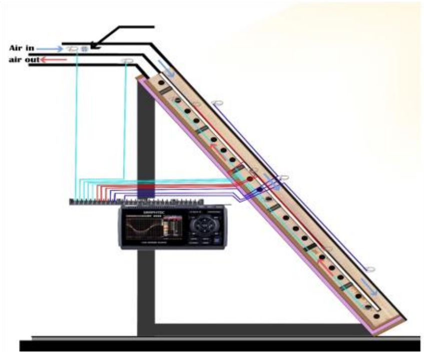

Fig. 3. The thermocouple installation location and the connection with the data logger

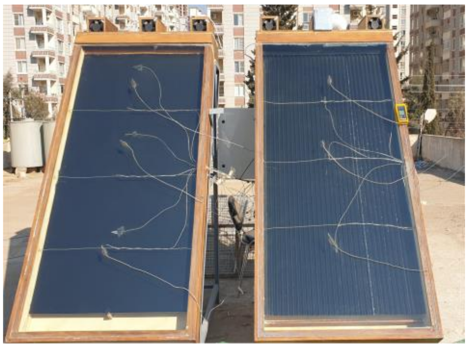

4a conventional SAH 4b improved SAH.
Fig. 4. Experimental rig

The complete system testing of SHA consists of a solar radiation sensor (pyranometer), an anemometer, a thermocouple, an axil fan to draw air into the system, and data logger device to get the required data. All of the testing equipment is listed in table 3.

Table 3: Experimental measuring tools

Name	Manufacturer	Model	Range	Accuracy
Solar radiation measurement	Beijing Ever Good electronic Company	TES -132	(0-2000) W/m^2	±5%
Anemometer		GM816	(0-30) m/s	±5%
Thermocouple	Vijay Heat Industries	Type K	(0-1250) °C	0.75% or ±2.2 °C
Fan	Zhejiang Fengdeng Electric Company	DS12038 AB H	0-184 m^3/h	—
Data logger	Graphtec American	GL840	20-200 channel	—

3.2. Comparison between conventional and improved SAH

Usually, the conventional solar air heater consists of a heat-absorbing flat plate that separates the upper and lower passages. It also contains fans to draw air into the system and raise the air temperature through the heat-absorbing flat plate and prepare a specific space, as, for the improved solar heater, a V-shaped corrugated plate at an angle of 60 degrees was employed. Wood baffles were added and phase -changing materials PCMs inside copper tubes and arranged horizontally along with the system. A barrier was added at the outlet of the solar air heater to control the percentage of air that will be recycled

3.3. Double pass SAHs with recycle

The air -flow meter is arranged as shown in figure 5. The new design of double-pass solar air heaters would help to divide the air -flowing conduit into two channels and inserts PCM into the lower channels with the baffles. The approach used in this study is experimentally for prediction of SAH efficiency. Prior to entering the lower subchannel, the mass flow rate and temperature of the incoming air are premixed with the recycling air -flow exiting the lower subchannel

Fig. 5. Air -flow double -pass SAHs with

3.4. Calibration of thermocouple

In order to make sure that all thermocouples have accurate reading, collecting data were compared to the thermometer readings. Both devices provide measurements for frozen water couple that has been placed in a metal container and subjected to a heat source. Gradually and by examining as shown in figure 6, we find a small discrepancy in the readings with the indication that the thermocouple responds to temperature changes faster than the thermometer and that the thermocouple reading is typically higher than the thermometer reading by around one degree Celsius. Every ten minutes, the thermocouple is read. How to wire it up to an Arduino and a computer.

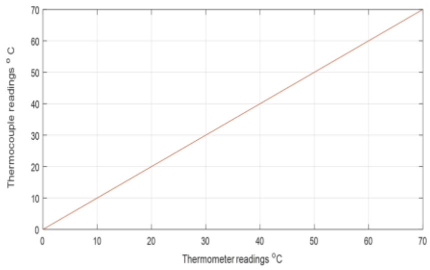

Fig.6. Calibration of thermocouple

3.5. Measurements uncertainty

Prior to the experiment, it is required to discover the factors that have a direct effect on the value of the thermal efficiency determined using the following relationship:

$$\eta = \left[\frac{\dot{m} cp (T_{out} - T_{in})}{I A_c} \right] \quad (5)$$

When $\dot{m}$ is the mass flow rate cp is the heat capacity of the air, T_{out}, T_{in} represented the outlet and inlet temperature of the SAH respectively. AS well as the I is the solar radiation and A_c is the cross sectional area air -flow. Since the amount of air -flowing, m, is a function of the density and volume of air -flowing:

$$m = f(\rho * Q)$$

And for a constant cross-sectional area Ac, and assuming that the properties of air remain constant, the temperature changes air measured in the experiment The amount of air -flowing is a function of velocity:

$$m = f(V)$$

To measure the uncertainty, the following equation can be used:

$$\frac{\omega_\eta}{\eta} = \sqrt{\left[\left(\frac{\omega_m}{m}\right)^2 + \left(\frac{\omega_{\Delta T}}{\Delta T}\right)^2 + \left(\frac{\omega_I}{I}\right)^2 \right]} \quad (6)$$

Where ($\frac{\omega_m}{m}$) denotes the percentage of partial error in measuring the volume of air -flowing, and $\frac{\omega_{\Delta T}}{\Delta T}$ denotes the percentage of partial error in measuring the difference in air temperatures, and $\frac{\omega_I}{I}$ denotes the percentage of partial error in detecting the intensity of solar radiation. The uncertainty of observed and calculated data for conventional and upgraded heaters is shown in Table 4 [20].

Table 4. Uncertainty measured and results of data for improved and conventional SAHs

SAH type	m (kg/s)	ΔT °C	I (w/m2)	%η	ω_m%	ω_η%
Conventional	0.037	10.81	690	27.56	0.185	1.95
Improved	0.037	13.57	521	48.43	0.185	3.44
Conventional	0.057	5.66	674	24.05	0.285	1.71
Improved	0.057	25.47	940	77.61	0.285	5.51

4. Experimental procedure

Before starting the practical part, it should be sure that there is no leakage at the joint of the SAHs as well as the tubes filled with paraffin wax. Also, check that the thermocouples are installed in the right location and that the devices are working properly. Experimental tests were conducted at Duhok Polytechnic University/ Technical College of Engineering in the Duhok governorate. By analyzing the recorded data, the relationship between air mass flow, useful heat gain, daily efficiency, and the difference between ambient temperature interring in the upper channel of SAH and the outlet temperature that is passing through the lower channel to warm cold space, that data can be obtained via a data logger device.

5. Result and discussion

The performance test of the conventional and improved solar air heater was carried out at the following mass flow rates (0.037, 0057, 0.077) kg/sec sience, that the air velocity for the three states of the mass flow rate which was previously mentioned were 2.7 m/s, 2 m/s, 1.3, m/s respectively. Table (5) shows the days for which data were recorded for the conventional solar air heater and improved solar air heater with recycle.

Table (5): The dates on which the experiments were carried out.

Type of SAH	Mass flow rate	Date
Conventional and improve with recycle	0.037 kg/s	15/02/2022 16/02/2022 17 /02/2022
Conventional and improve with recycle	0.057 kg/s	21/02/2022 24/02/2022 07/03/2022
Conventional and improve with recycle	0.077 kg/s	07/02/2022 12/02/2022 13/02/2022

Figure 7 is a curve for measuring the ambient temperature or the temperature of the air entering the conventional and improved solar air heaters, for three days 15,16, and17, February of 2022. From studying the figures, we conclude the temperature on the 17th of February has a maximum temperature value between the 15th and 16th of February. The results show that at one o'clock in the afternoon, it has the highest temperature measuring 18.73°C. Figure.7 shows the intensity of solar radiation for three days on February, 15, 16, and 17 of 2022. From the curves, it is clear that there is a difference in the amount of solar radiation falling on the earth from one day to another, and it increases with time, knowing that in the 17th of the month the maximum value among the other days was reached at 1067 W/m2 at the pick time of 1:00 p.m. Figure 8 shows the hourly various measured temperature of different elements for a conventional SAH on February 17, 2022 when the m= 0.037 kg/s.

Figure 9 shows that the temperatures of the flat plate, the cover of the solar SAH made of glass, the upper gap and the lower gap of collector increased with time, when it was noticed that the highest temperatures reached at 13.25 pm. The maximum values that have been recorded for T_{pl}, $T_{upper\ gap}$, $T_{lower\ gap}$, and T_g are found to be 77.53, 50.27, 54.49, and 48.57 °C respectively. In order to study the performance of improve SAH, figure 10 signalized the hourly various measured temperature of different elements on 17th of February 2022 when m=0.037 kg/s the maximum value of temperature for T_{pl}, $T_{upper\ gap}$, $T_{lower\ gap}$, T_{p1}, T_{p2}, $T_{\_p3}$ and T_g are found to be 91.35, 72.44, 74.54, 42.72,77.42, 76.64, and 56.46 respectively.

In figures (9 and 10), the experimental result shows that for improve SHA the difference temperature was enhancement and increased when was compared to the conventional heater. The maximum value of the difference temperature for improve and conventional heater were 55.95 °C at 13:35 and 38.91 at 13:25°C respectively.

Figure. 11 shows the hourly various measured temperature of different elements for a conventional SAH on February 24, 2022 when the (m= 0.057 kg/s). Figure 11 shows that the temperatures of the flat plate, the cover of the solar SAH made of glass, the upper gap and the lower gap of collector increased with time, when it was noticed that the maximum value of temperatures measured at 13.15 pm. The maximum values that have been recorded for T_{pl}, $T_{upper\ gap}$, $T_{lower\ gap}$, and T_g are found to be 51.48, 30.02, 36.77 and 39.29 °C respectively, as obviously seen in figure 11

In figures (11 and 12), the experimental result shows that for improve SHA the difference temperature was enhancement and increased when was compared to the conventional heater. The maximum value of the difference temperature when the mass flow rate for improve and conventional heater were 31.95 °C and 15.1°C. at 12:20 respectively.

In order to study the performance of improve SAH, figure 12 signalized the hourly various measured temperature of different elements on 24th February 2022 at mass flow rate (m=0.057 kg/s). The maximum values that have been recorded for T_{pl}, $T_{\_upper\ gap}$, $T_{\_lower\ gap}$, and T_g found to be 161.48, 40.78, 48.64, 43.73, 50.84, 55.87 and 40.76 °C respectively.

Figure 13, at a mass flow rate of 0.077 kg/sec, shows the temperature distribution of the different parts of the conventional SAH on February 7, 2022. The maximum values for have been recorded are T_{pl} =39.23, $T_{upper\ gap}$ =18.35, $T_{lower\ gap}$ =23.88, and T_g =30.02.

Figure. 14 shows the hourly various measured temperature of different elements for improve SAH on 7th February 2022 at mass flow rate (m=0.077 kg/s). The maximum temperature value at 12.45 p.m. of T_{pl}, $T_{upper\ gap}$, $T_{lower\ gap}$, T_{p1}, T_{p2}, T_{p3}, and T_g are found to be 50.2, 31.42, 36.81, 32.38 ,38.38, 42.1, and 35.84 °C respectively, as obviously seen in figure 13.

In figures (13 and 14) experimental result show that for improve SHA the difference temperature was enhancement and increased when was compared to the conventional heater. The maximum value of the difference temperature for improve and conventional heater were 30.94 °C and 13.43 at 12:20 respectively.

Figures 15, 16 and 17 show a comparison between the amount of useful heat in an improved and conventional heater. The maximum useful heat value for improve SAH were 1.68 kW, 1.86 and 2.57 kW at 0.037, 0.057 kg/s, and 0.077 kg/s respectively. While the useful heat values of the conventional heater were 0.87 kW, 0.97 kW, and 1.15 kW at 0.037, 0.057 kg/s, and 0.077kg/s respectively. As a result, the useful heat transfer can be increased when the mass flow rate is increased with time, and it was discovered that the improved heater by the PCM, recycle rate, V-shaped absorber plate, and baffles was more efficient than the conventional heater, including the absorber flat plat in DPSAH. It is clear that when the useful heat gain is increased, the efficiency of the SAH significantly increases.

Figure 18 explains the comparison of the daily efficiency for the improved SAH and conventional SAH on the various days in February 2022 (15, 16, and 17) at the mass flow rate of 0.037 kg/s. Daily efficiency of SAH is depends of the solar radiation, the result discovered that the daily efficiency of the improved heater has the maximum value of the conventional heater in three days of testing. This is due to the energy storage PCM, baffles, and recycling rate having good effects on the enhancement of the daily efficiency of the SAH and was increased significantly. On three days in February (15, 16, and 17), the daily efficiency for improving and conventional heater value was (84% and 45%), (86% and 46%), and (91% and 60%), respectively.

6. Conclusion

In the current research, 18 experiments were conducted on two different designs of a solar air heater at three values of the supplied air mass flow rate (0.037, 0.057, 0.077 kg/s) for the period from 12/2/2022 to 7/3/2022 under the weather conditions of Duhok city / Kurdistan - Iraq. The first design is for a conventional double-pass solar air heater and the other is for an improved double-pass solar air heater. The improved heater design has been modified by using 1- a corrugated V-shaped absorber plate at an angle of 60 instead of the flat plate in a conventional heater to increase the heat transfer area, 2- Wooden baffles in the heater lower pass to increase turbulence, 3- Copper tubes filled with phase -change material (paraffin wax) in the heater lower pass to store the excess heat and re-dispose it in the absence of solar radiation, and finally 4- Recycling part of the air leaving the heater (ratio of recycled air to total air is R=0.55) to raise the temperature of the supplied air in cold weather. These improvements led to an increase in the following: the supplied air temperature, the supplied useful heat and the daily efficiency. For example, the maximum values of useful heat transfer at mass flow rates (0.037, 0.057, and 0.077 kg/s are 1.68, 1.86, and 2.34 kW, respectively, and the daily efficiencies for improving and conventional heaters at a mass flow rate of 0.037 kg/s for February 15, 16, and 17 in 2022 were (84% and 45%), (86% and 46%), and (91% and 60%), respectively.

Nomenclature

A_c	Collector area (m2)
At	Cross section air of exit air the heater m2
$\dot{Q}_c$	Heat input through solar radiation (W)
$\dot{Q}_u$	Useful heat transfer (W)
I	Solar radiation intensity (W/m2)
$\dot{m}$	Mass flow rate (kg/s)
C_p	Specific heat capacity (kJ/kgK)
ΔT	Air temperature difference (°C)
T_{out}	Outlet temperature (°C)
T_{in}	Inlet air temperature (°C)
T_{pl}	Temperature of absorber plate (°C)
T_g	Glass cover temperature (°C)
$T_{upper\ gap}$	Upper gap air temperature (°C)
$T_{lower\ gap}$	Lower gap air temperature (°C)
T_p	Temperature of pipe (°C)

Abbreviations

SHA	Solar Air Heater
PCM	Phase Change Material
DPSAH	Double -Pass Solar Air Heater
FPSAH	Finned Plate Solar Air Heater

Greek symbol

η_{th}	Thermal efficiency of the solar air heater
ρ	Density of air (kg/m3)

REFERENCE

[1] F. Aissaoui, A. H. Benmachiche, A. Brima, D. Bahloul, and Y. Belloufi, "Experimental and theoretical analysis on thermal performance of the flat plate solar air collector," *Int. J. Heat Technol.*, vol. 34, no. 2, pp. 213–220, 2016, doi: 10.18280/ijht.340209.

[2] G. Cheng and L. Zhang, "Numerical simulation of solar air heater with V-groove absorber used in HD desalination," *Desalin. Water Treat.*, vol. 28, no. 1–3, pp. 239–246, 2011, doi: 10.5004/dwt.2011.1820.

[3] M. Sajawal, T. U. Rehman, H. M. Ali, U. Sajjad, A. Raza, and M. S. Bhatti, "Experimental thermal performance analysis of finned tube-phase change material based double -pass solar air heater," *Case Stud. Therm. Eng.*, vol. 15, p. 100543, 2019, doi: 10.1016/j.csite.2019.100543.

[4] A. El Khadraoui, S. Bouadila, S. Kooli, A. Guizani, and A. Farhat, "Solar air heater with phase change material: An energy analysis and a comparative study," *Appl. Therm. Eng.*, vol. 107, pp. 1057–1064, 2016, doi: 10.1016/j.applthermaleng.2016.07.004.

[5] E. Kabeel, A. Khalil, S. M. Shalaby, and M. E. Zayed, "Improvement of thermal performance of the finned plate solar air heater by using latent heat thermal storage," *Appl. Therm. Eng.*, vol. 123, pp. 546–553, 2017, doi: 10.1016/j.applthermaleng.2017.05.126.

[6] E. Kabeel, A. Khalil, S. M. Shalaby, and M. E. Zayed, "Experimental investigation of thermal performance of flat and v-corrugated plate solar air heaters with and without PCM as thermal

energy storage," *Energy Convers. Manag.*, vol. 113, pp. 264–272, 2016, doi: 10.1016/j.enconman.2016.01.068.

[7] P. C. Material, "Journal of engineering physics," *Int. J. Heat Mass Transf.*, vol. 6, no. 2, pp. 191–192, 1963, doi: 10.1016/0017-9310(63)90036-x.

[8] A. Koca, H. F. Oztop, T. Koyun, and Y. Varol, "Energy and exergy analysis of a latent heat storage system with phase change material for a solar collector," *Renew. Energy*, vol. 33, no. 4, pp. 567–574, 2008, doi: 10.1016/j.renene.2007.03.012.

[9] R. Moradi, A. Kianifar, and S. Wongwises, "Optimization of a solar air heater with phase change materials: Experimental and numerical study," *Exp. Therm. Fluid Sci.*, vol. 89, pp. 41–49, 2017, doi: 10.1016/j.expthermflusci.2017.07.011.

[10] V. V. Tyagi, A. K. Pandey, S. C. Kaushik, and S. K. Tyagi, "Thermal performance evaluation of a solar air heater with and without thermal energy storage An experimental study," *J. Therm. Anal. Calorim.*, vol. 107, no. 3, pp. 1345–1352, 2012, doi: 10.1007/s10973-011-1617-3.

[11] A. F. Sharol et al., "Effect of thermal energy storage material on the performance of double-pass solar air heater with cross-matrix absorber," *J. Energy Storage*, vol. 51, no. July, p. 104494, 2022, doi: 10.1016/j.est.2022.104494.

[12] R. Karwa and B. K. Maheshwari, "Heat transfer and friction in an asymmetrically heated rectangular duct with half and fully perforated baffles at different pitches," *Int. Commun. Heat Mass Transf.*, vol. 36, no. 3, pp. 264–268, 2009, doi: 10.1016/j.icheatmasstransfer.2008.11.005.

[13] E. Bensaci, A. Moummi, F. J. Sanchez de la Flor, E. A. Rodriguez Jara, A. Rincon-Casado, and A. Ruiz-Pardo, "Numerical and experimental study of the heat transfer and hydraulic performance of solar air heaters with different baffle positions," *Renew. Energy*, vol. 155, pp. 1231–1244, 2020, doi: 10.1016/j.renene.2020.04.017.

[14] H. Olfian, A. Z. Sheshpoli, and S. S. Mousavi Ajarostaghi, "Numerical evaluation of the thermal performance of a solar air heater equipped with two different types of baffles," *Heat Transfer*, vol. 49, no. 3, pp. 1149–1169, 2020, doi: 10.1002/htj.21656.

[15] R. Bakari, "Heat Transfer Optimization in Air Flat Plate Solar Collectors Integrated with Baffles," *J. Power Energy Eng.*, vol. 06, no. 01, pp. 70–84, 2018, doi: 10.4236/jpee.2018.61006.

[16] D. Ho, Y. E. Tien, and H. Chang, "Performance improvement of a double-pass V-corrugated solar air heater under recycling operation," *Int. J. Green Energy*, vol. 13, no. 15, pp. 1547–1555, 2016, doi: 10.1080/15435075.2016.1206004.

[17] D. Ho, H. Chang, R. C. Wang, and C. S. Lin, "Performance improvement of a double-pass solar air heater with fins and baffles under recycling operation," *Appl. Energy*, vol. 100, pp. 155–163, 2012, doi: 10.1016/j.apenergy.2012.03.065.

[18] O. Hamdoon, "A review of solar air heaters: techniques for thermal performance enhancement," *Al-Rafidain Eng. J.*, vol. 25, no. 2, pp. 46–59, 2020, doi: 10.33899/rengj.2020.128374.1065.

[19] A. Mermoud, "PVSyst – Logiciel Photovoltaïque," ISE, University of Geneva (2012). 2012, Accessed: Mar. 04, 2022. [Online]. Available: https://www.pvsyst.com/.

[20] J. P. Holman, *Experimental Methods For Engineers*, Natl Inst Science Communication Dr Ks Krishnan Marg, New Delhi, India, 1966.

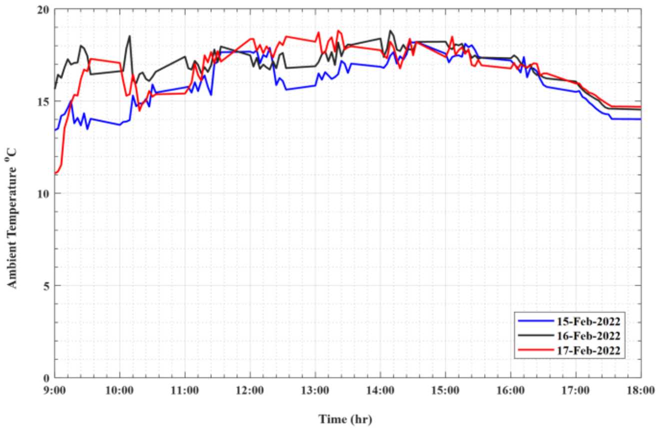

Fig.7. Measured of the ambient temperature in different day on February month

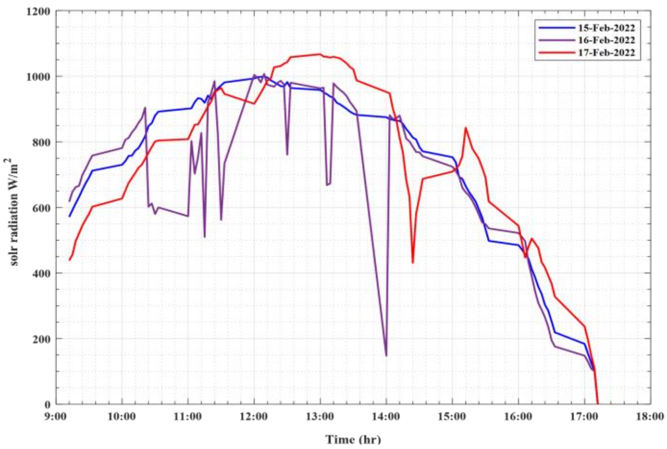

Fig.8. Variation of solar radiation (W/m^2) in February

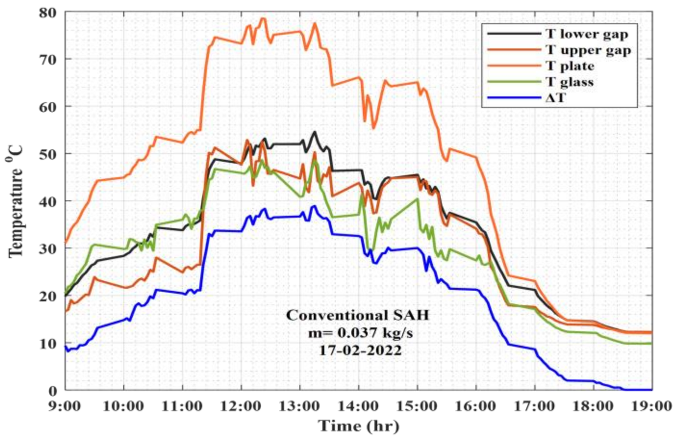

Fig.9. Measured temperature of different elements for a conventional SAH (hr)

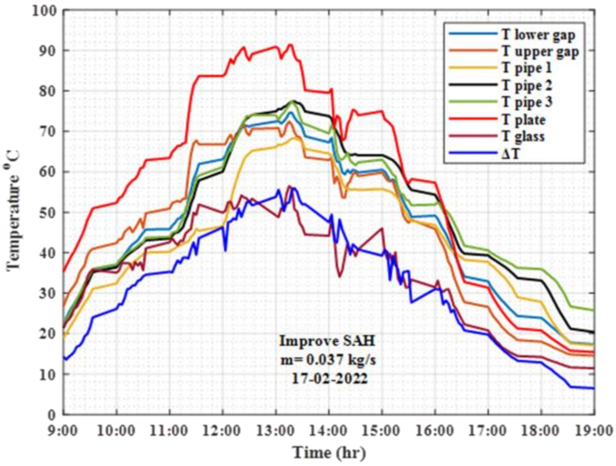

Fig.10. Measured different elements for an improve SAH (hr)

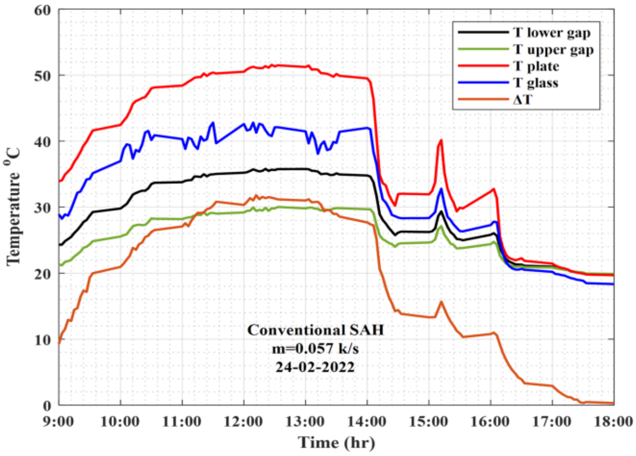

Fig.11. Illustrate the temperature of different elements for a conventional SAH with time at mass flow rate 0.057 kg/s

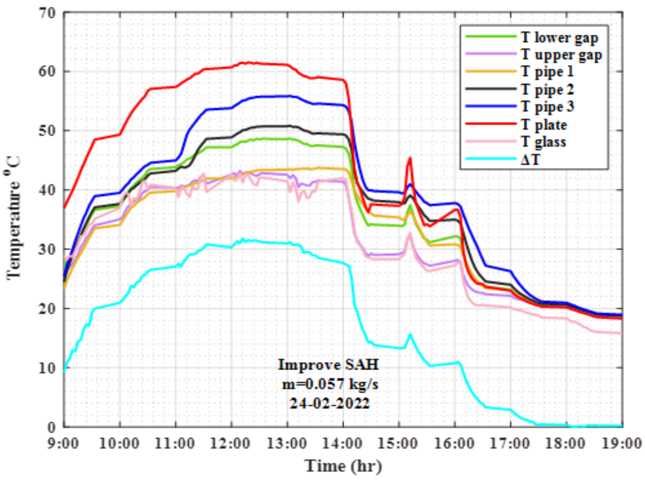

Fig.12. Illustrate the temperature of different elements for an improve SAH vs. time at mass flow rate 0.057 kg/s

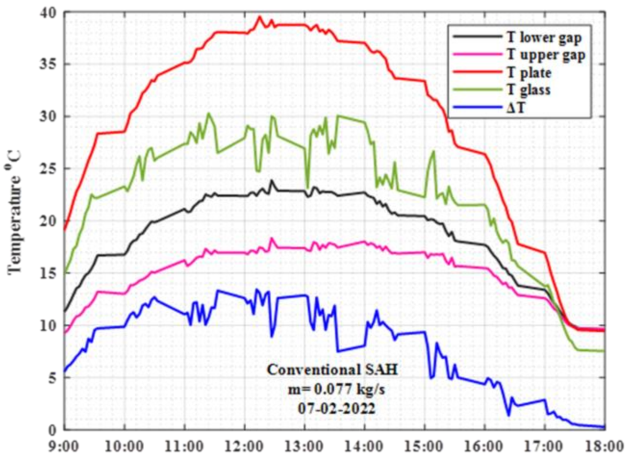

Fig.13. Measured temperature of different elements for a conventional collector when the mass flow rate is 0.077 with time (hr)

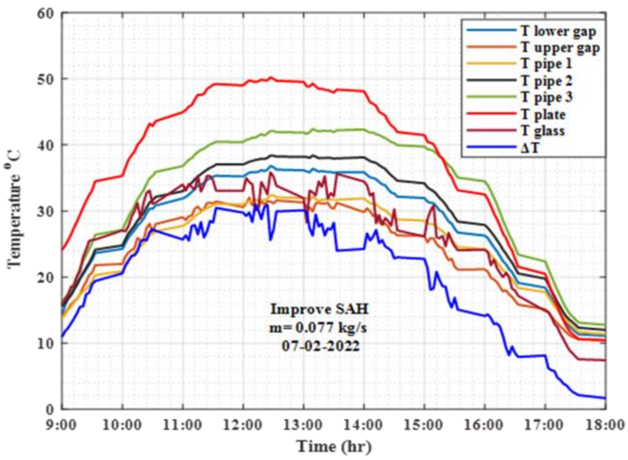

Fig.14. Illustrate the temperature of different elements for an improve SAH vs. time at mass flow rate 0.077 kg/*s*

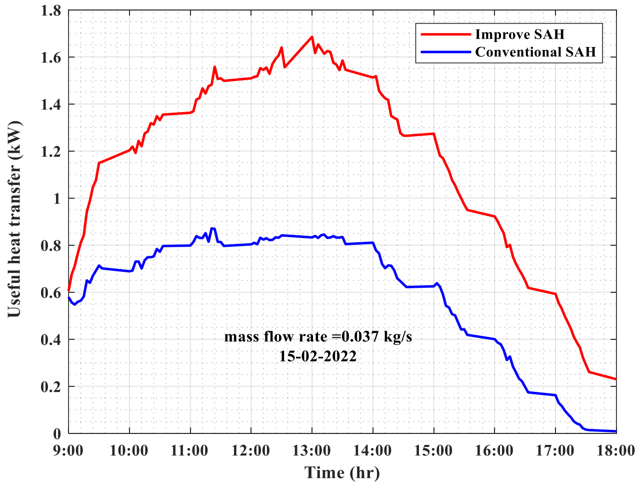

Fig. 15. Comparison of useful heat transfer between improved and conventional SAHs

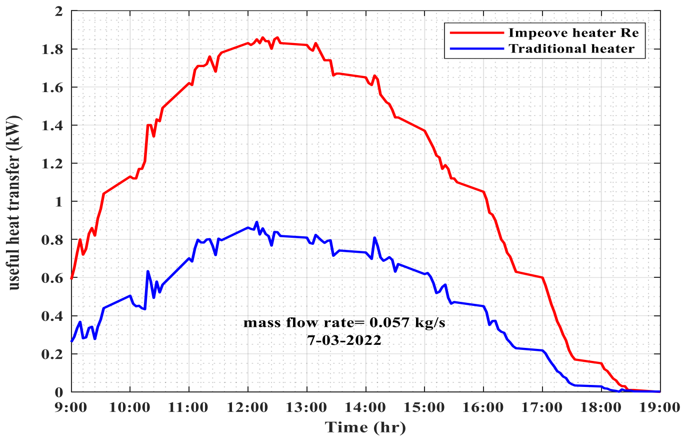

Fig. 16. Comparison of useful heat transfer between improved and traditional heaters

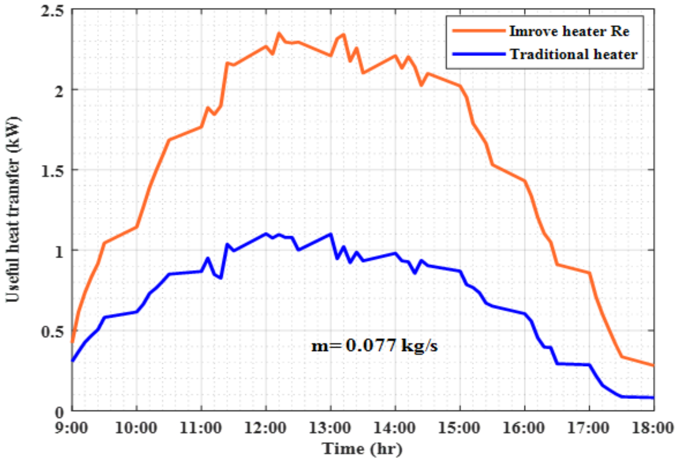

Fig. 17. Comparison of useful heat transfer between improved and traditional heaters in 12-02-2022

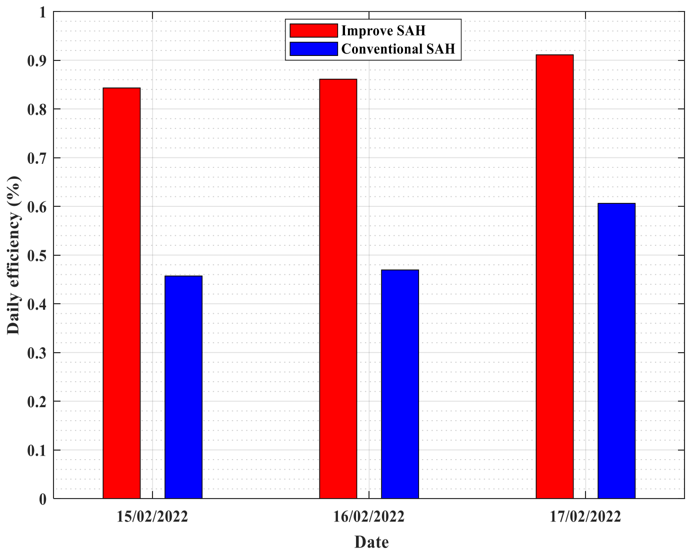

Fig. 18. Daily efficiency on different days at a mass flow rate of 0.037 kg/s

فحص تجريبي لسخان هواء شمسي مزدوج المسار مع لوح مموج على شكل حرف V ، ومواد متغيرة الطور وحواجز تحت عملية إعادة التدوير

عمر محمد حمدون*
eng.omar.m.hamdoon@uomosul.edu.iq

إبراهيم بابكرعلي *
ibrahim.ababakr@gmail.com

جامعة الموصل - كلية الهندسة – قسم الهندسة الميكانيكية - موصل - العراق*
جامعة دهوك بوليتكنيك - الكلية التقنية للهندسة - قسم هندسة الطاقة -دهوك -العراق**

تاريخ الاستلام:21-09-2022 استلم بصيغته المنقحة:25-10-2022 تاريخ القبول:15-11-2022

الملخص

تقدم الورقة الحالية عملاً تجريبيًا تم تنفيذه لمراقبة أداء سخان الهواء الشمسي المحسن ومقارنته بأداء سخان الهواء الشمسي المسطح المزدوج الممر التقليدي. تشمل التحسينات التي تمت إضافتها استخدام لوح مموج على شكل حرف V بزاوية 60 درجة ، وإضافة حواجز خشبية في الممر السفلي واستخدام مواد متغيرة الطور PCM بالإضافة إلى ظروف إعادة تدوير الهواء. تم تصميم السخان واختباره في ظل الظروف الجوية السائدة في محافظة دهوك (خط العرض 36 ° 52 '1.52 "شمالاً وخط الطول 42 ° 59' 18.42" شرقاً) في إقليم كردستان العراق. مادة PCM المتغيرة الطور هي شمع البارافين. أظهرت النتائج التي تم جمعها أن التحسينات التي تمت إضافتها إلى سخان الهواء الشمسي أدت إلى تحسين الأداء بشكل ملحوظ عند قيم تدفق كتلة مختلفة (0.037 ، 0.057 ، 0.077 كجم / ثانية). على سبيل المثال ، كان التحسن في نقل الحرارة المفيد حوالي 56٪ عند 0.057 كجم / ثانية.

الكلمات الدالة:

سخان الهواء الشمسي ، PCM ، إعادة التدوير ، لوح امتصاص مموج على شكل V.